Biochemistry

New Concepts in Biochemistry

Divalent Cations Stabilize Unstacked Conformations of DNA and RNA by Interacting with Base Π Systems[†]

Lori McFail-Isom, Xiuqi Shui, and Loren Dean Williams*

School of Chemistry & Biochemistry, Georgia Institute of Technology, Atlanta, Georgia 30332-0400

Received September 11, 1998; Revised Manuscript Received October 15, 1998

ABSTRACT: Nucleic acid structure, stability, and reactivity are governed substantially by cations. We propose that magnesium and other biological inorganic ions unstack bases of DNA and RNA. This unstacking function of cations opposes their previously accepted role in stabilizing DNA and RNA duplexes and higher assemblies. We show that cations interact favorably with π-systems of nucleic acid bases. These cation-π interactions require access of cations or their first hydration shells to faces of nucleic acid bases. We observe that hydrated magnesium ions located in the major groove of B-DNA pull cytosine bases partially out from the helical stack, exposing π-systems to positive charge. A series of critical cation-π interactions contribute to the stability of the anticodon arm of yeast-tRNA^{phe}, and to the magnesium core of the Tetrahymena group I intron P4−P6 domain. The structural consequences of divalent cation-π interactions are clearly distinct from, and some cases in opposition to, cation−electron lone pair interactions. These observations of cation-π interactions suggest a number of new mechanistic roles for cations in DNA bending, DNA−protein recognition, base-flipping, RNA folding, and catalysis.

We propose that magnesium and other biological inorganic ions interact with the faces of DNA and RNA bases, causing the bases to unstack. This unstacking function opposes the previously accepted role of cations in stabilizing DNA and RNA duplexes. The results described here indicate that divalent cations and their first hydration shells seek faces of nucleic acid bases, interacting favorably with π-systems.

Cation-π interactions between amino acid side chains are known to contribute to the stability of protein native states (*1−3*). For example a continuous (cation-π-)$_n$ stack composed of Lys-Tyr-Arg-Phe-Arg-Trp-Lys (KYRFRWK) is observed in the X-ray structure of the human growth hormone/receptor complex (*4*). Cation-π interactions also contribute to the stability of protein−ligand complexes. The X-ray structure of acetylcholine esterase (*5*) confirms Dougherty's model in which the cationic amine of acetylcholine is stabilized by the π-system of a tryptophan (*6, 7*). Similarly, in a complex with UMP/CMP kinase, the π-system of an adenine stacks on the cationic center of an arginine (*8*).

Cation-π interactions are thought to be among the strongest noncovalent interactions (*9*). Experimental gas-phase enthalpies for binding of monovalent cations to benzene range from 38 (Li$^+$) to 9 kcal/mol [N(CH$_3$)$_4$$^+$]. The favorable energetic nature of cation-π interactions is supported by statistical clustering of phenyl rings around onium groups (*10*) within the Cambridge Structural Database (*11*). The interaction is generally dominated by electrostatics, but charge transfer, polarization, and other components contribute

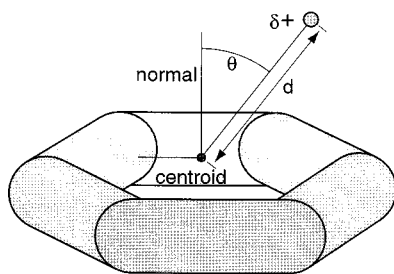* Author to whom correspondence should be addressed.

FIGURE 1: Geometric definitions used for describing cation-π interactions.

in some cases. As discussed by Ma and Dougherty (*9*), favorable interactions between aromatic systems and cations do not necessarily involve hydrogen bonds or formally charged species. For example the methyl groups of $N(CH_3)_4^+$ interact favorably with π-systems.

Significant positive charge is carried on the first-shell water molecules of divalent cations such as $Mg(OH_2)_6^{2+}$. We propose that $Mg(OH_2)_6^{2+}$ engages in cation-π interactions with DNA and RNA bases. We have screened the nucleic acid database (*12*) for structures stabilized by such cation-π interactions. The results of the screen confirm the hypothesis. Here we describe divalent cation-π interactions of Mg-$(OH_2)_6^{2+}$ with distorted B-DNA, yeast-tRNA^{phe}, and the tetrahymena group I intron P4−P6 domain.

METHODS

The screening of three-dimensional structures for interactions such as hydrogen bonding, cation-π, etc. requires geometrical definitions of interactions. For example a hydrogen bond is "observed" in a crystal structure if a hydrogen bond donor and an acceptor are within a certain distance and related by certain angles. Geometric definitions for cation-π interactions are established here from the geometry of cation-π pairs within the KYRFRWK stack of the human growth hormone/receptor complex (PDB entry 3HHR). For each cation-aromatic pair within that stack, two parameters were determined: a distance d and an angle θ (Figure 1). The distance d is between the positions of the cationic atom and the centroid of the adjacent aromatic ring. The angle θ is defined by the positions of the cation, the ring centroid, and the base normal, as shown in Figure 1. The angle θ is always positive and less than 180°. The upper limits of the angle θ and distance d, beyond which the interaction is considered to be insignificant, were established by adding 2σ to the averages within the KYRFRWK stack. A cation-π interaction is inferred here when d is less than or equal to 5.2 Å and θ is less than or equal to 52°, and the line from ion to ring centroid is not obstructed by other atoms, with their boundaries determined by van der Waals radii. The geometric criteria for cation-π interactions defined here are consistent with, but are more conservative than, previously established criteria (*10*) derived from analysis of the small molecule crystallographic database.

The definition of a cationic atom is somewhat arbitrary. The definition might be limited to atoms with formal positive charge. For example certain nitrogen atoms of amino acid side chains carry a charge of −1.0 or −0.33 electrons. Alternatively an expanded definition could include carbon atoms bound to formally charged nitrogen atoms. The
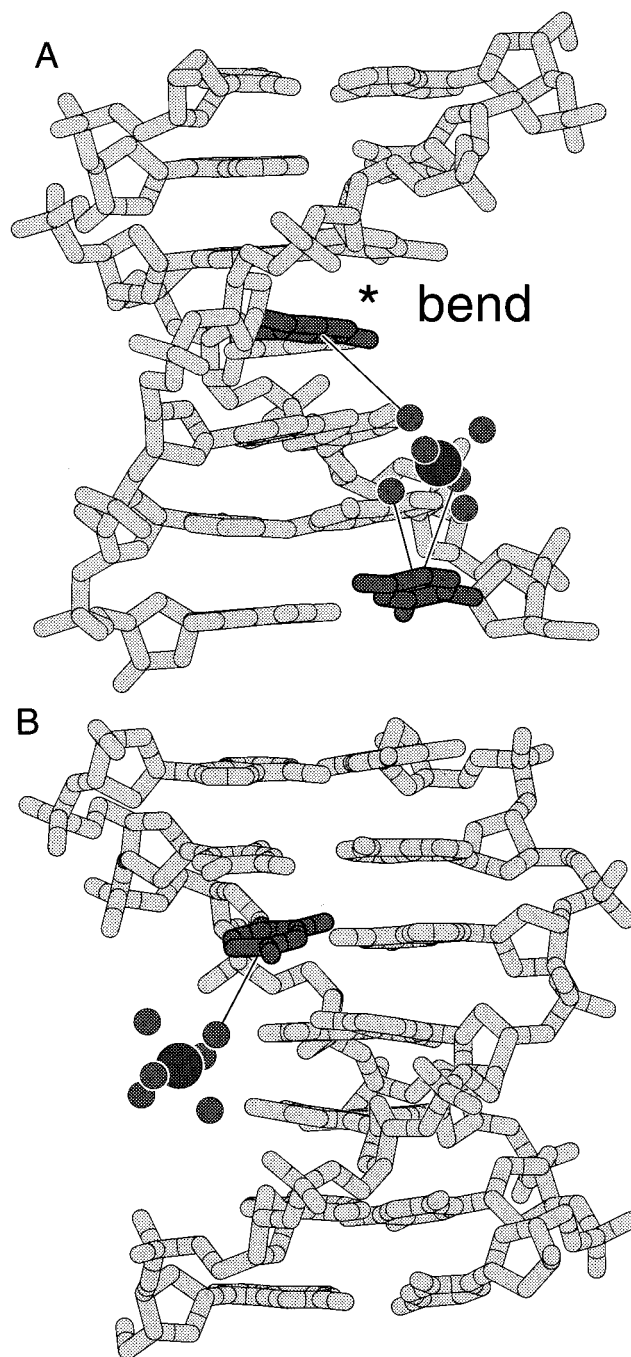

FIGURE 2: Cation-π interactions in the major groove of distorted B-DNA. Lines indicate cation-π interactions of DNA bases with $Mg(OH_2)_6^{2+}$. The DNA is represented in stick form. The bases that engage in cation-π interactions are cytosines (shaded). $Mg(OH_2)_6^{2+}$ is represented by circles, with the radius of Mg^{2+} greater than that of first-shell water oxygens: (A) a portion of DNA dodecamer duplex d(CGCGAATTCGCG); and (B) a portion of decamer d(CGATCGATCG).

averages and upper limits of the distance d and the angle θ were computed by both of these definitions and were found to be invariant. The inclusion or exclusion of the partially charged carbon atoms had a negligible effect on the averages or upper limits.

Cation-π interactions were detected by geometric analysis of our 1.4 Å structure of the dodecamer d(CGCGAAT-TCGCG) (NDB entry BDL084, ref 13). Additional B-DNA-magnesium complexes within the Nucleic Acid Database
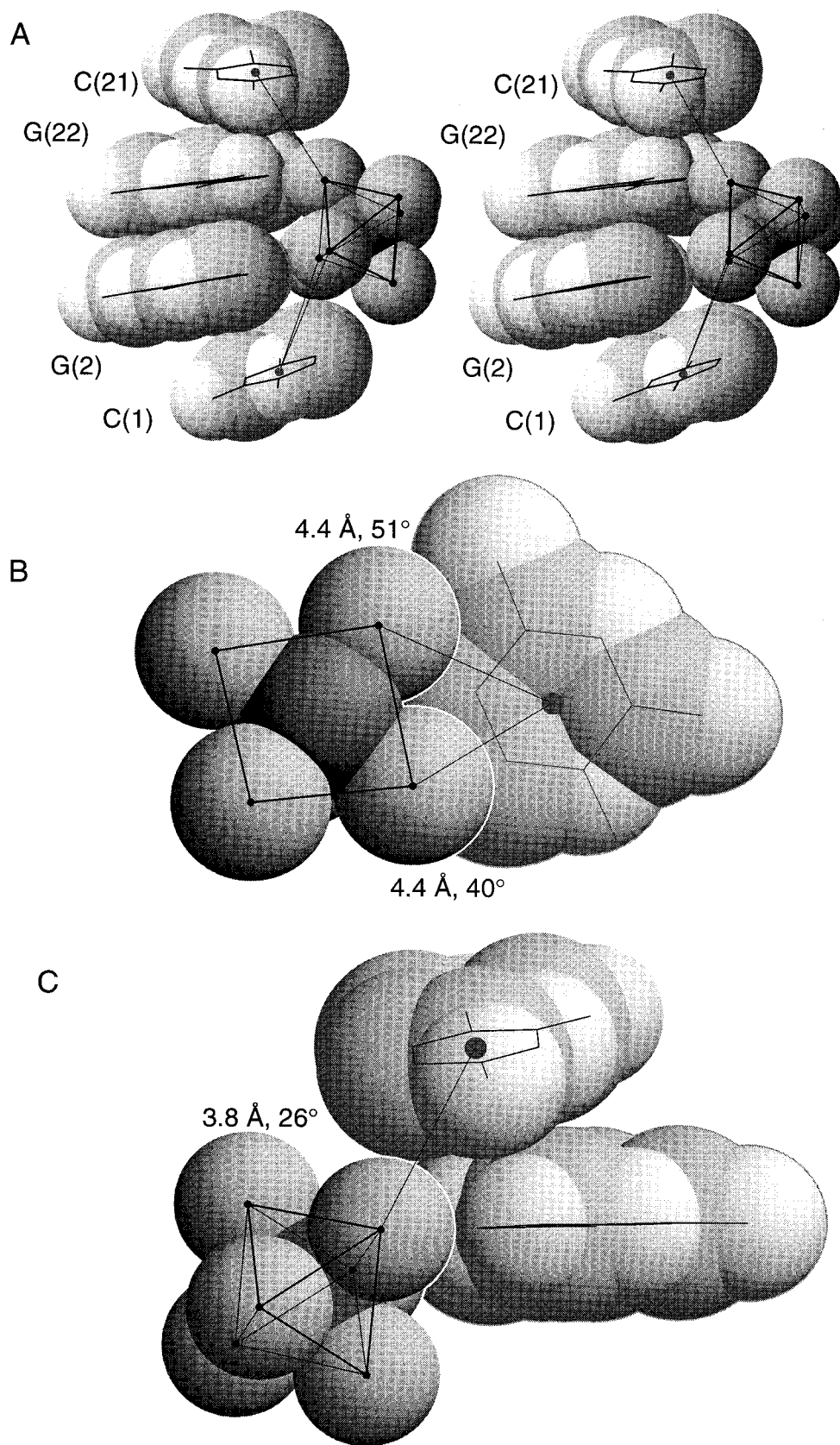
FIGURE 3: Space-filling views of cation-π interactions of DNA bases with $Mg(OH_2)_6^{2+}$. Cation-π interactions between shell water molecules of $Mg(OH_2)_6^{2+}$ and π-systems of cytosines are indicated by lines. Base centroids are indicated by solid circles. The water molecules that surround the magnesium ion are connected to illustrate the octahedra. Atoms are shaded by type with Mg (dark) > first-shell oxygen > carbon > oxygen > nitrogen (light). (A) Stereoview of a portion of the DNA dodecamer duplex d(CGCGAATTCGCG) showing the $Mg(OH_2)_6^{2+}$ in the major groove. The cup-shaped cavity formed by the DNA to accommodate the $Mg(OH_2)_6^{2+}$ is apparent. Only the bases that interact with the hydrated magnesium complex are shown. Residues C(1) and C(21) interact via cation-π interactions. Residues G(2) and G(22) interact via conventional lone pair interactions. (B) The same complex viewed along the normal of base C(21). Two water molecules are omitted for clarity. (C) The complex formed by decamer d(CGATCGATCG). The destacking of C(5) is apparent.

Table 1: Cation-π Contacts of Mg(OH$_2$)$_6$$^{2+}$ with DNA Bases

residue	ring	ion[a]	d^b (Å)	θ^c (deg)
[d(CGCGAATTCGCG)]$_2$				
cytosine 1	pyrimidine	Mg	5.4	51
		WO2	4.4	51
		WO5	4.4	40
cytosine 21	pyrimidine	Mg	6.8	47
		WO1	4.9	51
[d(CGATCGATCG)]$_2$				
A:cytosine 5	pyrimidine	Mg	5.1	42
		W05	3.8	26

[a] Ion indicates either magnesium ion or an outer-sphere water molecule. [b] Distance is from ring centroid to ion or first-shell water molecule. [c] Angle is between base plane normal and line from ion to ring centroid.

were screened. B-DNA structures with resolution worse than 1.5 Å or containing drugs, chemical modifications, or mismatches were excluded. Three structures qualified for analysis. Two do not meet the geometric criteria and lack cation-π interactions. The 1.5 Å structure of Grzeskowiak and co-workers [d(CGATCGATCG) (NDB entry BDJ025, ref 14) contains a hydrated magnesium complex within the major groove that does engage in cation-π interactions with the DNA.

A search of the NDB produced two yeast-tRNA^{phe} structures with resolution of 2.7 Å or higher. The highest-resolution yeast-tRNA^{phe} structure (NDB entry TRNA10, resolution 2.5 Å) lacks first-shell water molecules around the magnesium ions. Therefore the geometric screen was performed on the next highest-resolution structure (NDB entry TRNA04, resolution 2.7 Å).

The model of the P4−P6 domain of the tetrahymena ribozyme (NDB entry URX053) is derived from relatively low-resolution diffraction data. This model lacks first-shell waters around most magnesium ions. However this structure is an inviting target for analysis because of the large number of divalent cations within the interior of the RNA fold. Our analysis of this structure is artificially limited, by the lack of first-shell water molecules in the model, to cation-π interactions between magnesium ions and RNA bases.

RESULTS

DNA Complexes with Divalent Cations Are Stabilized by Cation-π Interactions. Cation-π interactions of Mg(OH$_2$)$_6$$^{2+}$ with nucleic acid bases are "observed" here by geometry. An Mg(OH$_2$)$_6$$^{2+}$ is located in the major groove of the high-resolution B-DNA dodecamer d(CGCGAATTCGCG) (Figures 2 and 3). The Mg(OH$_2$)$_6$$^{2+}$ engages in conventional outer-shell interactions with electron donors (N7 and O6 positions) at the edges of two guanine bases. The Mg-(OH$_2$)$_6$$^{2+}$ also engages in cation-π interactions with two cytosine bases. These cytosine bases, one on either side of the magnesium ion, appear to be pulled partially out from the helical stack. This shift of the bases exposes π-systems to the positive charge of the magnesium ion and its outer-shell water molecules (Table 1). The cup-shaped binding cavity formed by the DNA is clearly evident in Figure 3. The strongest interaction, as indicated by the shortest contact (4.4 Å) and least acute angle (40°), involves first-shell water molecule W05 and terminal cytosine C(1). That same base interacts with an additional first-shell water molecule (W02)

Table 2: Cation-π Contacts of Mg(OH$_2$)$_6$$^{2+}$ and Cobalt Hexamine with RNA Bases

residue	ring	ion[a]	d^b (Å)	θ^c (deg)
Anticodon Arm of Yeast-tRNA^{phe}				
		Mg 80		
pseudouracil 39	pyrimidine	WO4	5.1	31
	pyrimidine	WO5	4.9	48
Y 37	imidazole	WO2	5.0	40
	imidazole	WO4	3.1	52
uracil 33	pyrimidine	WO1	4.5	46
adenine 36	imidazole	WO1	4.5	42
	imidazole	WO4	5.0	10
P4-P6 Domain of Tetrahymena Group 1 Ribozyme^d				
adenine 171	imidazole	Mg 14	4.9	45
adenine 172	imidazole	Mg 16^e	6.0	6
adenine 173	imidazole	Mg 16	4.8	47
guanine 110	imidazole	Mg 25^e	5.9	28
adenine 139	pyrimidine	Mg 7^e	5.3	28
guanine 200	imidazole	Mg 27^e	6.3	49
guanine 118	imidazole	Mg 27^e	6.3	57
adenine 146	imidazole	Co 1^f	5.9	39
	imidazole	N2 1	4.8	27
	imidazole	N6 1	4.9	44
guanine 174	imidazole	Co 2^f	6.0	38
	imidazole	N3 2	4.7	52
	imidazole	N6 2	5.0	32
guanine 175	imidazole	Co 2^f	5.6	65
	imidazole	N2 2	4.4	51

[a] Ion indicates either magnesium ion or its outer-sphere water molecule, or cobalt or its outer-sphere amine. [b] Distance from ring centroid to ion. [c] Angle is between base plane normal and line from ion to ring centroid. [d] In the A chain. Nearly identical interactions are observed in the B chain. [e] These magnesium ions fall slightly outside our criteria but have been included because outer-sphere interactions would presumably fall within the criteria if water molecules were included in the model. [f] Distance d exceeds criteria, suggesting that this ion is engaged in outer-sphere, but not inner-sphere, cation-π interactions.

but at a more acute angle (4.4 Å, 51°). At the other end of the binding cup, cytosine C(21) is in contact with W01 (4.9 Å, 49°).

The high-resolution B-DNA decamer d(CGATCGATCG) (NDB entry BDJ025, ref 14) contains a Mg(OH$_2$)$_6$$^{2+}$ within the major groove. This Mg(OH$_2$)$_6$$^{2+}$ engages in conventional outer-shell interactions with electron donors and in cation-π interactions with a flanking cytosine (Figures 2 and 3). One of the first-shell water molecules (W05) interacts with the face of residue C(5) (Table 1). The DNA is distorted so that the face of the pyrimidine is exposed to the cationic water molecule. The contact of C(5) with W05 is short (3.8 Å), and the water molecule is located close to the base normal, with an angle θ of only 26°.

RNA complexes with divalent cations are stabilized by cation-π interactions. The three-dimensional structure of yeast-tRNA^{phe} (*15*) contains several magnesium ions. Only the magnesium ion within the anticodon arm engages in cation-π interactions. This ion forms a total of seven cation-π interactions, involving four tRNA bases (Table 2, Figure 4). The first-shell water molecule WO4 interacts with π-systems of three bases (PSU39, YG37, and A36).

Within the tetrahymena group I intron P4−P6 domain, four magnesium ions are located less than 5 Å from centroids of adenine imidazole rings (Table 2). Even in the current model (*16*), which lacks many first-shell magnesium water molecules, our structural criteria for cation-π interactions are met in many instances. Approximately one-third of mag-
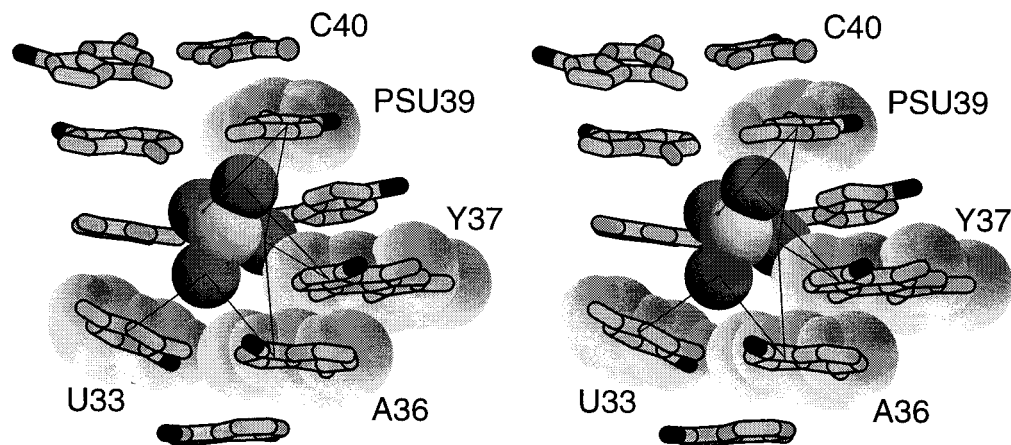
FIGURE 4: Stereoview of a portion of the yeast-tRNA^{phe} anticodon arm. The $Mg(OH_2)_5^{2+}$ is represented in space fill. First-shell water molecules are darker than the magnesium ion. The bases are represented in stick, with shaded C1' atoms. The van der Waal surfaces are represented only for the RNA bases that engage in cation-π interactions. Cation-π interactions are represented by lines. The 5-methyl group of C40 is represented by a circle. The ribophosphodiester backbone and one first-shell water molecule of $Mg(OH_2)_5^{2+}$ are omitted for clarity.
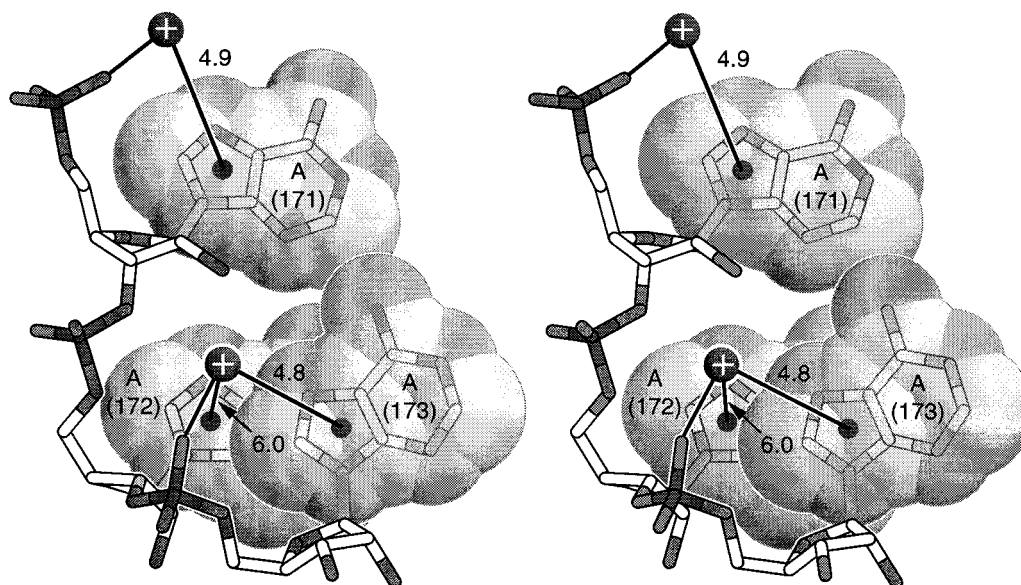

FIGURE 5: Space-filling stereoview of a portion of the P4−P6 domain of the tetrahymena group 1 ribozyme. The RNA is represented in stick. The van der Waal surfaces of the RNA bases are also shown. Cation-π and cation-lone pair interactions are indicated by lines. Magnesium ions are represented by circles containing plus signs. Atoms are shaded by type with P (dark) > O > N > C (light). Distances are in Angstroms. Magnesium ion 14 interacts with the π-system of adenine 171 and with a lone pair of a phosphate oxygen. Magnesium ion 16 interacts with the π-systems of adenine 172 and adenine 173 and with a lone pair of a phosphate oxygen of adenine 173.

nesium ions observed in the structure interact with faces of RNA bases (Table 2). Several are located directly ($\theta < 10°$) over centers of imidazole rings. Three magnesium ions interact simultaneously with two π-systems. We also observe that cobalt hexamine engages in first-shell cation-π interactions with RNA bases (Table 2).

DISCUSSION

Nucleic acid structure, stability, and reactivity are governed substantially by cations. Hard monovalent cations bind preferentially in diffuse "ion atmospheres" and confer nonspecific stability to nucleic acid secondary and tertiary structures (*17*). Preferential localization of monovalent cations within the minor groove of AT-tracts appears to cause DNA bending and minor groove narrowing (*18*).

Divalent cations often interact specifically and can promote DNA bending (*19, 20*), fold large RNA molecules (*21, 22*),

serve as ribozyme cofactors (*23*), etc. In the current model, divalent cations form complexes with nucleic acid base and backbone atoms exclusively by binding to electron lone pair donors (*24*). In that model divalent cations bind by inner-sphere and outer-sphere coordination to edges of nucleic acid bases and phosphate oxygens.

Here we propose a new model in which magnesium and other divalent cations interact not only with electron lone pairs but with π-systems of nucleic acid bases. $Mg(OH_2)_6^{2+}$ forms complexes with *edges and faces* of nucleic acid bases. The π-system interactions, like electron lone pair interactions, can involve either inner-sphere or outer-sphere coordination.

Although interactions of inorganic cations with π-systems of nucleic acids have not been previously described or postulated, in a complex with UMP/CMP kinase, the π-system of an adenine stacks on the cationic center of an arginine (*8*). Cation-π interactions are clearly evident from
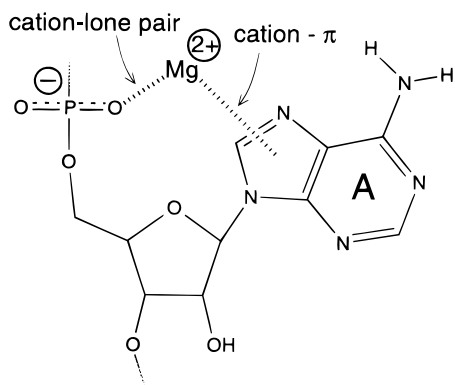
FIGURE 6: Cyclic structure in which a magnesium ion interacts simultaneously with both a lone pair of a phosphate oxygen and the π electrons of the imidazole ring.

our redetermination (*13*) of the structure of the "Dickerson dodecamer", d(CGCGAATTCGCG) (*25, 26*). The high resolution (1.4 Å) of the new B-DNA structure allows accurate determination of DNA, conformation, solvent, and counterion interactions. In the high-resolution structure, partial unstacking and exposure of the faces of two cytosine bases to the cationic charge are clear indication that the DNA is distorted by cation-π interactions.

The location of the magnesium ion in d(CGCGAAT-TCGCG) is adjacent to, and probably contributes to, the "dodecamer bend" (*27*). The other end of the dodecamer, where a spermine is bound to the major groove, is linear. Spermine, with more dispersed charge than magnesium, should interact much more weakly with π-systems. Thus divalent cations and polyamines should have different effects on nucleic acid structure, in part from differential interactions with π-systems.

The anticodon arm of yeast-tRNA^{phe} (*15*) contains an extensive and intricate network of cation-π interactions linking a Mg(OH$_2$)$_5^{2+}$ with RNA bases (Table 2, Figure 4). Magnesium is known to bind tightly to the anticodon arm, inducing a structural transition (*28*). The magnesium affinity of the anticodon arm of yeast-tRNA^{phe} is highly dependent on cytosine methylation at position C40 (*28*). However Mg-(OH$_2$)$_5^{2+}$ does not interact directly with C40 in the crystal structure. Cation-π interactions are a possible mechanism for modulation of magnesium affinity by methylation at C40, providing a relatively direct connection between the magnesium ion and the methyl group of C40. The position and charge distribution of PSU39 are undoubtedly influenced by the methylation of C40 (Figure 4).

The central structural scaffold of the tetrahymena group I intron P4−P6 domain contains a core of magnesium ions (*29, 30*). Ionic cores may explain the divalent ion requirement for folding of large ribozymes (*21*). Unlike B-DNA, full exposure of base faces of the folded ribozyme allows extensive and intimate cation-π contacts (Figure 5). The ionic core interacts pervasively with the faces of RNA bases. Several magnesium ions interact simultaneously with two π-systems. An adenosine-platform (*16*), formed by sequentially adjacent adenosine residues that lie side-by-side in a pseudo-base pair, is stabilized by an extended cation-π system (Figure 5). Strong forces and substantial energies must characterize these interactions.

In RNA, Mg(OH$_2$)$_6^{2+}$ appears to prefer π-systems of purines over pyrimidines, and imidazole rings over the pyrim-

idine rings, although the data set is small. Within the group I intron P4−P6 domain, four magnesium ions are located less than 5 Å from the centroids of adenine imidazole rings. A common motif is the cyclic structure shown in Figure 6, where a magnesium ion interacts with both a lone pair of the phosphate and the π electrons of the imidazole ring.

Summary. The observation of cation-π interactions here suggests a number of new mechanistic roles for cations in DNA bending (*19, 20*), strand separation (*24*), DNA−protein recognition, base flipping (*31*), RNA folding (*21, 22*), and catalysis (*23*). The structural consequences of cation-π-interactions are distinct from, and in opposition to, those of cation−electron lone pair interactions. Cation-π induced base displacement could be a general mechanism of magnesium-dependent recognition of DNA. The cation-π interactions observed at dCG steps, and the structural consequences of these interactions, may be common features of DNA-divalent cation complexes. dGC steps are partial recognition elements for many magnesium-dependent restriction enzymes and other sequence-specific DNA-binding proteins.

REFERENCES

1. Burley, S. K., and Petsko, G. A. (1986) *FEBS Lett. 203*, 139−143.
2. Karlin, A. (1993) *Curr. Opin. Neurobiol. 3*, 299−309.
3. Mitchell, J. B., Nandi, C. L., McDonald, I. K., Thornton, J. M., and Price, S. L. (1994) *J. Mol. Biol. 239*, 315−331.
4. de Vos, A. M., Ultsch, M., and Kossiakoff, A. A. (1992) *Science 255*, 306−312.
5. Raves, M. L., Harel, M., Pang, Y. P., Silman, I., Kozikowski, A. P., and Sussman, J. L. (1997) *Nat. Struct. Biol. 4*, 57−63.
6. Dougherty, D. A., and Stauffer, D. A. (1990) *Science 250*, 1558−60.
7. Stauffer, D. A., and Karlin, A. (1994) *Biochemistry 33*, 6840−9.
8. Scheffzek, K., Kliche, W., Wiesmuller, L., and Reinstein, J. (1996) *Biochemistry 35*, 9716−9727.
9. Ma, J., and Dougherty, D. (1997) *Chem. Rev. 97*, 1303−1324.
10. Verdonk, M., Boks, G., Kooijman, H., Kanters, J., and Kroon, J. (1993) *J. Comput.-Aided Mol. Des. 7*, 173−182.
11. Allen, F. H., Davies, J. E., Galloy, J. J., Johnson, O., Kennard, O., Macrae, C. F., Mitchell, E. M., Mitchell, G. F., Smith, J. M., and Watson, D. G. (1991) *J. Chem. Inf. Comput. Sci. 31*, 187−204.
12. Berman, H. M., Olson, W. K., Beveridge, D. L., Westbrook, J., Gelbin, A., Demeny, T., Hsieh, S. H., Srinivasan, A. R., and Schneider, B. (1992) *Biophys. J. 63*, 751−759.
13. Shui, X., McFail-Isom, L., Hu, G. G., and Williams, L. D. (1998) *Biochemistry 37*, 8341−8355.
14. Grzeskowiak, K., Yanagi, K., Prive, G. G., and Dickerson, R. E. (1991) *J. Biol. Chem. 266*, 8861−8883.
15. Sussman, J. L., Holbrook, S. R., Warrant, R. W., Church, G. M., and Kim, S.-H. (1978) *J. Mol. Biol. 123*, 607.
16. Cate, J. H., Gooding, A. R., Podell, E., Zhou, K., Golden, B. L., Szewczak, A. A., Kundrot, C. E., Cech, T. R., and Doudna, J. A. (1996) *Science 273*, 1696−1699.
17. Anderson, C. F., and Record, M. T., Jr. (1995) *Annu. Rev. Phys. Chem. 46*, 657−700.
18. Shui, X., McFail-Isom, L., Sines, C., VanDerveer, D., and Williams, L. D. (1998) *Biochemistry 37* (in press).
19. Diekmann, S., and Wang, J. C. (1985) *J. Mol. Biol. 186*, 1−11.
20. Laundon, C. H., and Griffith, J. D. (1987) *Biochemistry 26*, 3759−3762.
21. Celander, D. W., and Cech, T. R. (1991) *Science 251*, 401−407.
22. Pyle, A. M. (1993) *Science 261*, 709−714.
23. McConnell, T. S., Herschlag, D., and Cech, T. R. (1997) *Biochemistry 36*, 8293−8303.

24. Kazakov, S. A. (1996) in *Bioorganic Chemistry: Nucleic Acids* Hecht, S. M., Ed.) pp 244−287, Oxford University Press, New York.

25. Wing, R., Drew, H., Takano, T., Broka, C., Takana, S., Itakura, K., and Dickerson, R. E. (1980) *Nature 287*, 755−758.

26. Drew, H. R., Wing, R. M., Takano, T., Broka, C., Itakura, K., and Dickerson, R. E. (1981) *Proc. Natl. Acad. Sci. U.S.A. 78*, 2179−2183.

27. Dickerson, R. E., Goodsell, D. S., and Neidle, S. (1994) *Proc. Natl. Acad. Sci. U.S.A. 91*, 3579−3583.

28. Chen, Y., Sierzputowska-Gracz, H. R. G., Everett, K., and Agris, P. (1993) *Biochemistry 32*, 10249−10253.

29. Cate, J. H., Gooding, A. R., Podell, E., Zhou, K., Golden, B. L., Kundrot, C. E., Cech, T. R., and Doudna, J. A. (1996) *Science 273*, 1678−1685.

30. Cate, J. H., Hanna, R. L., and Doudna, J. A. (1997) *Nat. Struct. Biol. 4*, 553−558.

31. Demple, B. (1995) *Curr. Biol. 5*, 719−721.